

PAPER • OPEN ACCESS

## Measurements of the quantitative lateral analytical resolution at evaporated aluminium and silver layers with the JEOL JXA-8530F FEG-EPMA

To cite this article: D Berger and J Nissen 2018 *IOP Conf. Ser.: Mater. Sci. Eng.* **304** 012002

View the [article online](#) for updates and enhancements.

You may also like

- [Comprehensive investigation of Li-based novel quaternary Heusler  \$\text{LiTiPdZ}\$  \( \$Z = \text{Al, Ga, In}\$ \) compounds for thermoelectric performance](#)  
Lokanksha Suktel and Sapan Mohan Saini
- [Investigations of half-Heusler compounds  \$\text{CrScZ}\$  \( \$Z = \text{P, As, Sb}\$ \): a density functional theory study](#)  
R Ahmad and N Mehmood
- [IrCrMnZ \( \$Z = \text{Al, Ga, Si, Ge}\$ \) Heusler alloys as electrode materials for MgO-based magnetic tunneling junctions: a first-principles study](#)  
Tufan Roy, Masahito Tsujikawa and Masafumi Shirai

**ECS**  
The  
Electrochemical  
Society  
Advancing solid state &  
electrochemical science & technology

**DISCOVER**  
how sustainability  
intersects with  
electrochemistry & solid  
state science research

# Measurements of the quantitative lateral analytical resolution at evaporated aluminium and silver layers with the JEOL JXA-8530F FEG-EPMA

D Berger and J Nissen

Technische Universität Berlin, Zentraleinrichtung Elektronenmikroskopie ZELMI,  
Straße des 17. Juni 135, 10623 Berlin, Germany

E-mail: dirk.berger@tu-berlin.de; joerg.nissen@tu-berlin.de

**Abstract.** The studies in this paper are part of systematic investigations of the lateral analytical resolution of the field emission electron microprobe JEOL JXA-8530F. Hereby, the quantitative lateral resolution, which is achieved in practise, is in the focus of interest. The approach is to determine the minimum thickness of a metallic layer for which an accurate quantitative element analysis in cross-section is still possible. Previous measurements were accomplished at sputtered gold ( $Z = 79$ ) layers, where a lateral resolution in the range of 140 to 170 nm was achieved at suitable parameters of the microprobe. To study the  $Z$ -dependence of the lateral resolution, now aluminium ( $Z = 13$ ) resp. silver ( $Z = 47$ ) layers with different thicknesses were generated by evaporation and prepared in cross-section subsequently by use of a focussed Ga-ion beam (FIB). Each layer was analysed quantitatively with different electron energies. The thinnest layer which can be resolved specifies the best lateral resolution. These measured values were compared on the one hand with Monte Carlo simulations and on the other hand with predictions from formulas from the literature. The measurements fit well to the simulated and calculated values, except the ones at the lowest primary electron energies with an overvoltage below  $\sim 2$ . The reason for this discrepancy is not clear yet and has to be clarified by further investigations. The results apply for any microanalyser – even with energy-dispersive X-ray spectrometry (EDS) detection – if the probe diameters, which might deviate from those of the JEOL JXA-8530F, at suitable analysing parameters are considered.

## 1. Introduction

In contrast to the qualitative lateral analytical resolution, where the analytical issue is to recognise the smallest features by element distributions, the quantitative lateral analytical resolution is of great significance for the determination of the accurate element composition of small features. The first attempt to define the quantitative resolution are measurements of the rise of the X-ray intensity of an element as edge profile at the interface of two different materials from 1 to 99 % X-ray intensity. Measurements at an Au-Si interface resulted in a quantitative lateral resolution of 90 nm [1]. Since resolution measurements by edge profiles depends on the adjacent elements, it is more useful to determine the quantitative resolution from the smallest feature for which an accurate quantitative element analysis is still feasible. The limiting parameters hereby are mainly the mean atomic number  $Z$  of the feature elements, the primary electron energy  $E_0$  and the beam diameter which might be rather large for low  $E_0$  and suitable beam currents (figure 1). To study the  $Z$ - and  $E_0$ -dependence of the



analytical lateral resolution, features were generated by vapour deposition of metallic layers with different atomic number and then analysed quantitatively by varying the primary electron energy.

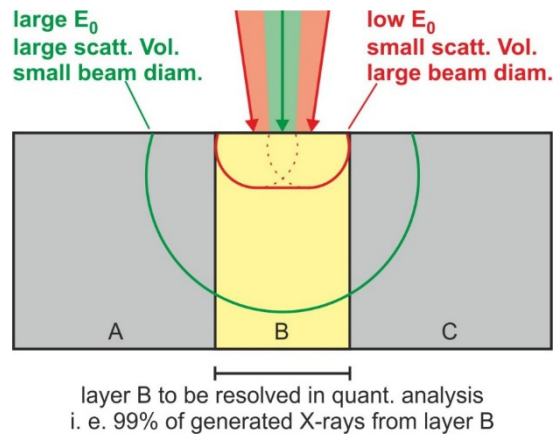


**Figure 1.** Influence of primary electron energy  $E_0$  and beam diameter on X-ray emitting volume and quantitative lateral analytical resolution.

## 2. Experimental and results

### 2.1. Deposition and preparation of the layers

For the experimental determination of the quantitative analytical lateral resolution under different measurement conditions, aluminium layers with different thicknesses (3850, 940, 445, 345, 280 and 260 nm) were generated by evaporation on silicon wafer substrates. The cross-sectional preparation of the specimens was done first by cleaving and then by cutting an about 50 - 100  $\mu\text{m}$  wide cross-section with a rough (30 kV, 21 nA) focussed Ga-ion beam (FEI Helios Nano Lab600 FIB). Second, free spaces are milled adjacent to the cross-section, if necessary, to avoid fluorescence effects, see figure 2.

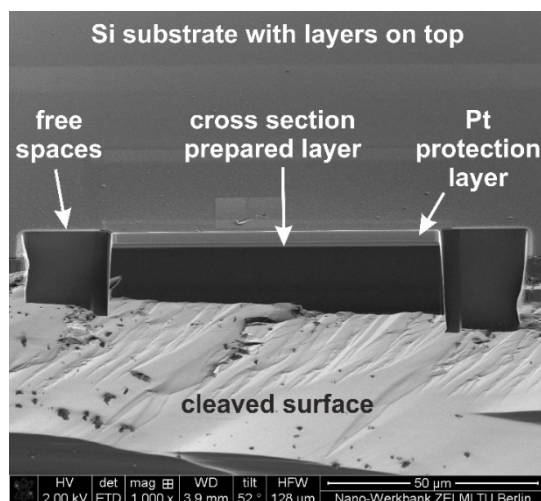


**Figure 2.** SEM image of a cleaved Si substrate with ion-beam prepared cross-section surface and the free spaces. The evaporated Al layer on top of Si is too thin to be resolved in this image.

In the last preparation step a gentle ion beam (30 kV, 90 pA) is used to polish the cross-section surface with low implantation of Ga into the Al layer. The cross-section polishing process requires a mechanical protection layer consisting of Ga, Pt and C which is apparent on top of the aluminium layer. Figure 3 shows high resolution SE-images of the cross-section of the 6 layers.

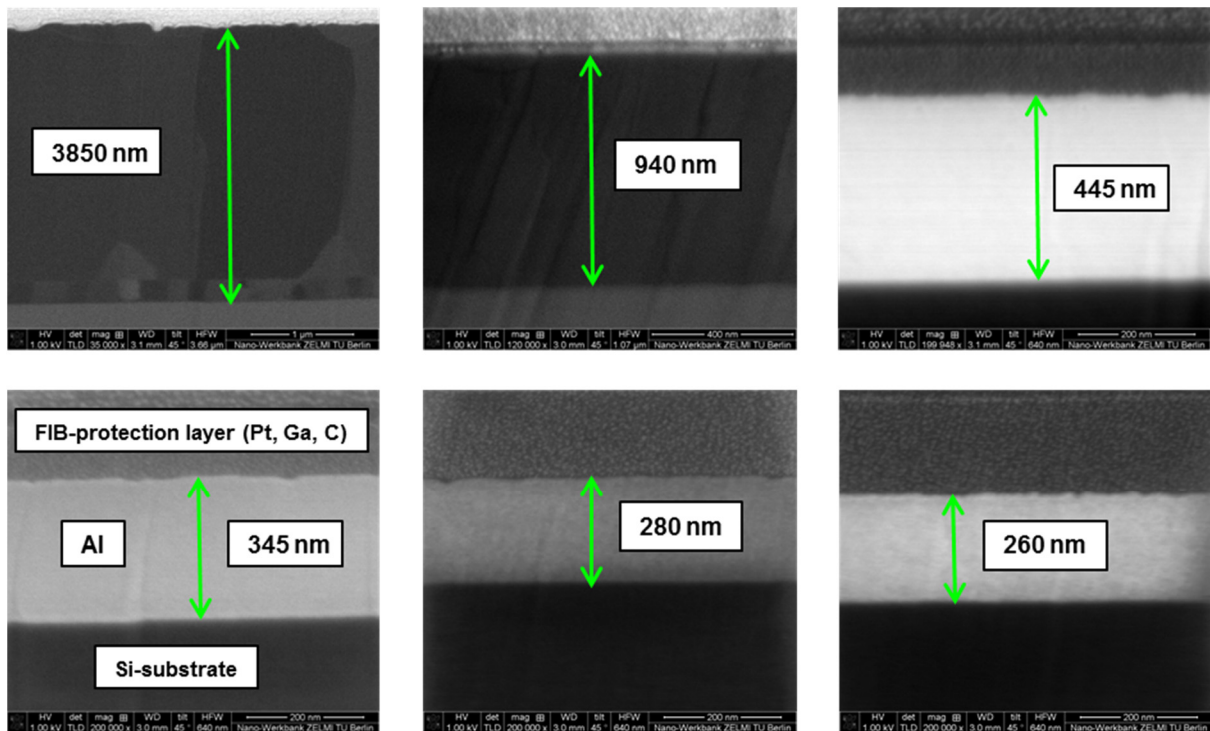


**Figure 3.** Cross-section images of the test specimens with different aluminium layers from 3850 to 260 nm thickness.

The preparation of the silver layers was accomplished in the same way as the aluminium layers with one difference. To avoid fluorescence effects in the Si-substrate and the FIB protection layer, two additional palladium layers were deposited, adjacent to the silver layer. Ag-L $\alpha$  X-ray with energy of 2.984 keV cannot excite Pd-L $\alpha$  X-ray by fluorescence due to the higher critical ionisation energy of Pd-L $\alpha$  X-ray at 3.172 keV. Figure 4 shows the layer structure with the 3 thinnest silver layers.

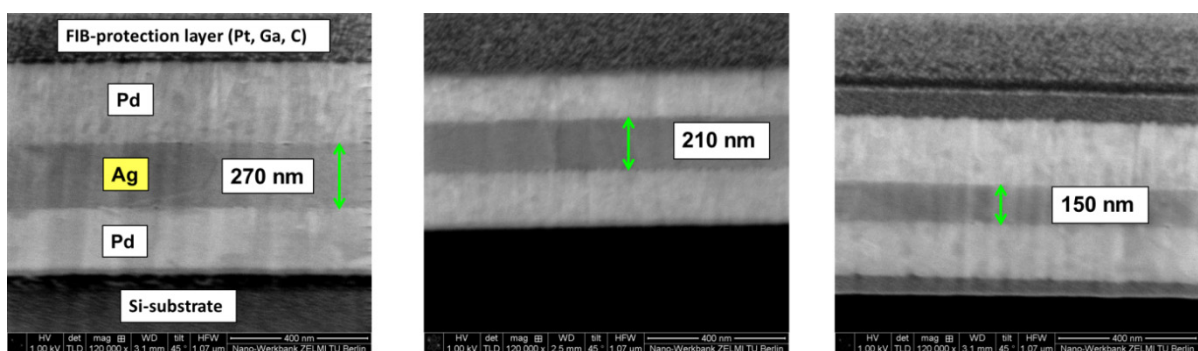


**Figure 4.** Cross-section images of the test specimens with different silver layers from 270 to 150 nm thickness.

The density of both the Al and the Ag-layers were determined by the weighing method [2] to  $(2.68 \pm 0.02) \text{ g/cm}^3$  and  $(10.4 \pm 0.1) \text{ g/cm}^3$  respectively. These density values are close to the bulk material densities indicating that the evaporated layers are not porous. Finally, the density values are verified by analysing quantitative measurements with the thin film software STRATAGEM.

## 2.2. Measured quantitative lateral resolution

Each test specimen is analysed quantitatively for different electron energies using the 3850 nm Al layer and the 2000 nm Ag layer as standard respectively. By applying an appropriate probe current, the beam diameter is chosen to be smaller than about 50 nm, see figure 1. Beam diameters are determined in correspondence with ISO/TS 24597 by the analysis of the contrast profile in images of gold insulars on carbon [1]. Wavelength-dispersive X-ray spectrometry (WDS) measurements are done with the Al  $K\alpha$ -line on the TAP crystal and the Ag  $L\alpha$ -line on the PET crystal. The acquisition time (20 s for the peak and 10 s for the background) and the beam currents are chosen to minimise drift effects at a reasonable counting statistics.

Table 1 summarizes the results of the element quantification for the aluminium layers at the electron energies 15, 8, 7, 5, 4 and 3 keV. Even lower energies are not practical due to the decreasing image quality, which makes the beam adjustment more difficult, and due to the too low overvoltage. To get sufficient X-ray intensity, the appropriate overvoltage to excite Al- $K\alpha$  X-ray (critical ionisation energy: 1.559 keV) should not be below  $\sim 2$  [3].

**Table 1.** Results of the quantitative measurements of the aluminium layers in wt% Al.

Al layer thickness [nm]	15 keV	8 keV	7 keV	5 keV	4 keV	3 keV
3850 (Reference)	100.00	100.00	100.00	100.00	100.00	100.00
940	/	97.82	100.08	99.96	100.16	99.92
445	/	/	89.76	99.68	99.75	99.95
345	/	/	/	95.18	99.89	99.87
280	/	/	/	/	97.93	99.61
260	/	/	/	/	/	98.95
Beam diameter $d_0$ [nm]	<b>30</b>	<b>43</b>	<b>33</b>	<b>38</b>	<b>45</b>	<b>52</b>
Probe current [nA]	<b>5</b>	<b>5</b>	<b>1</b>	<b>1</b>	<b>1</b>	<b>1</b>

The values in the table are the averages of 10 measurements in weight percent aluminium (wt% Al). A quantification result is expected to be accurate if it is in the range of  $(100.0 \pm 0.5) \%$ , indicating that the source volume of the emitted X-rays is completely inside the Al layer within statistical fluctuations. The 280-nm layer is the thinnest which can be resolved (99.61 wt% Al). Thus, for aluminium a lateral quantitative resolution in the range of 260 to 280 nm is achieved at 3 keV electron energy.

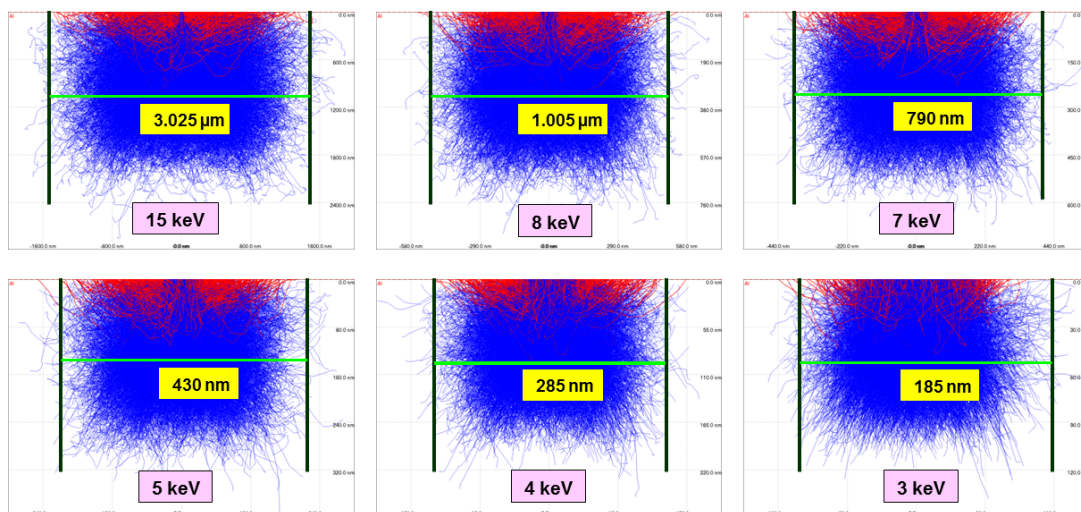
The quantification results for silver are shown in table 2. Here, the lowest practical electron energy to excite Ag- $L\alpha$  X-ray (critical ionisation energy: 3.352 keV) is 5 keV (overvoltage:  $5/3.352 = 1.49$ ). The thinnest layer, for which an accurate analysis is still feasible here, is 210 nm (100.29 wt% Ag). The best resulting lateral resolution for silver is the range of 150 to 210 nm at 5 keV.

**Table 2.** Results of the quantitative measurements of the silver layers in wt% Ag.

Ag layer thickness [nm]	15 keV	8 keV	7 keV	6 keV	5 keV
2000 (Reference)	100.00	100.00	100.00	100.00	100.00
870	98.77	99.82	100.08	99.96	100.16
270	/	96.21	99.82	99.65	100.28
210	/	/	96.78	99.71	100.29
150	/	/	/	/	95.79
Beam diameter $d_0$ [nm]	30	43	33	35	38
Probe current [nA]	5	5	1	1	1

### 2.3. Monte Carlo simulation of the quantitative lateral resolution

The electron scattering in aluminium and silver for electron energies between the primary energy (15, 8, 7, 6, 5, 4 and 3 keV) and the critical ionisation energy (1.559 keV for Al-K and 3.352 keV for Ag-L) is simulated with the programme CASINO (version 2.48) [4]. Figures 5 and 6 show the resulting plots of the electron paths of primary electrons (blue) and backscattered electrons (red). For the determination of the quantitative analytical resolution 99 % of the 10,000 simulated trajectories were taken into account by counting by hand. The width of the interaction volume of these 99 % of electron paths is defined as the simulated lateral resolution, see indications in figures 5 and 6. The self-absorption of Al-K $\alpha$  in Al and Ag-L $\alpha$  in Ag is proved to be very small so that the range of the electron paths is a very well measure for the range of emitted X-rays.

**Figure 5.** Monte Carlo simulations of scattered electrons in Al with different electron energies.

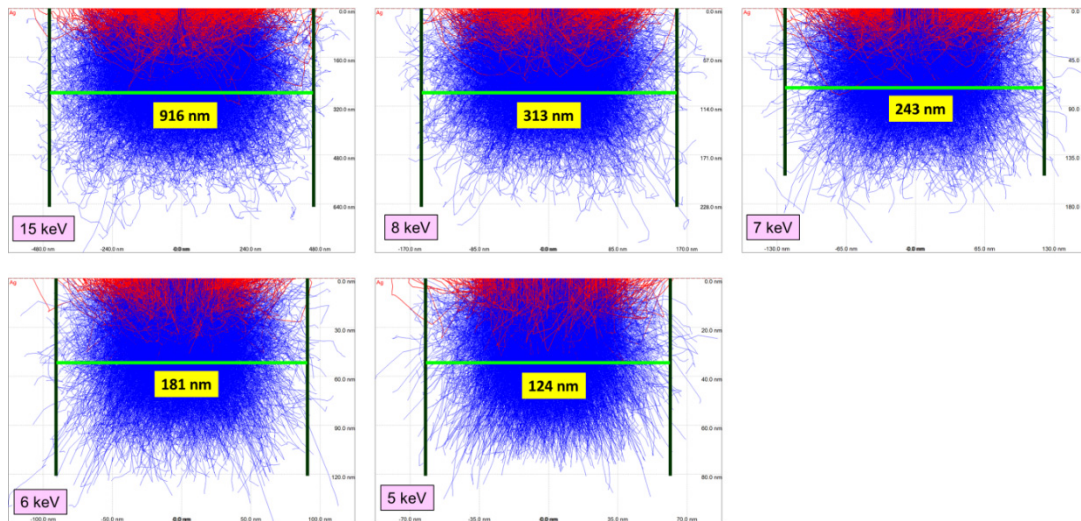


**Figure 6.** Monte Carlo simulations of scattered electrons in Ag with different electron energies.

#### 2.4. Calculation of the quantitative lateral resolution

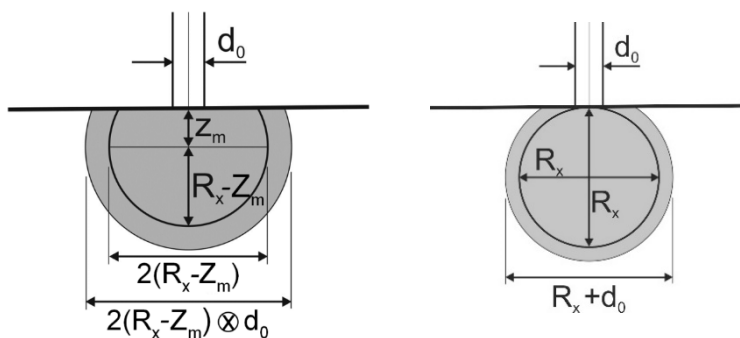
In the last step the quantitative lateral resolution  $R_S$  was calculated firstly by the eq. (1) from Merlet and Llovet [5] and secondly by the eq. (2) from Willich and Bethke [6]:

$$R_S = \sqrt{4 \cdot (R_x - Z_m)^2 + d_0^2} \quad (1)$$

$$R_S = R_x + d_0 \quad (2)$$

with  $R_S$  is the lateral analytical resolution in nm,  $R_x$  is the ionisation range,  $d_0$  the beam diameter and  $Z_m$  the depth of the maximum of the X-ray depth distribution [7].

Figure 7 illustrates that equation (1) is based on the convolution of the interaction volume (its radius is estimated by  $R_x - Z_m$ ) with the beam diameter which is obtained from measurements. In contrast, eq. (2) regards a linear sum between the ionisation range and the beam diameter.

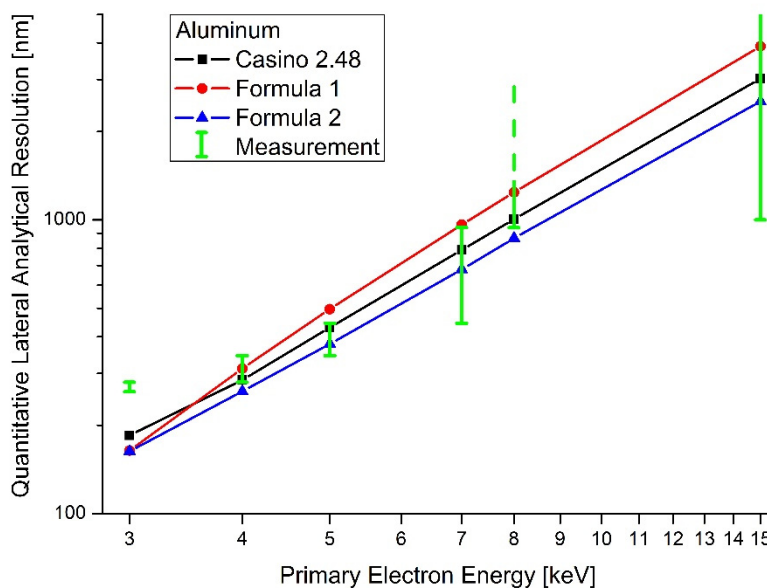


**Figure 7.** Schematic illustration of parameters specifying the lateral resolution in eqs. (1) and (2).

For aluminium table 3 and figure 8 represent the comparison of the simulated, calculated and measured lateral resolutions as a function of the excitation energy  $E_0$ . Since the measurements are based on 6 specimens with different layer thickness, the measured lateral resolutions are specified as a range.

**Table 3.** Comparison of simulated, calculated and measured quantitative lateral resolutions for Al and different primary electron energies.

Electron energy	Lateral resolution from MC simulation [nm]	$R_x$ [nm]	$Z_m$ [nm]	Calculated lateral resolution $R_s$ with formula (1) [nm]	Calculated lateral resolution $R_s$ with formula (2) [nm]	Measured lateral resolution [nm]
15 keV	3025	2499	548	3902	2529	940-3850
8 keV	1005	823	202	1242	866	940-3850
7 keV	790	645	163	965	678	445-940
5 keV	430	340	92	497	378	345-445
4 keV	285	216	61	313	261	280-345
3 keV	185	111	164	164	163	260-280

**Figure 8.** Comparison of the simulated, calculated and measured quantitative lateral resolutions for Al and different primary electron energies.

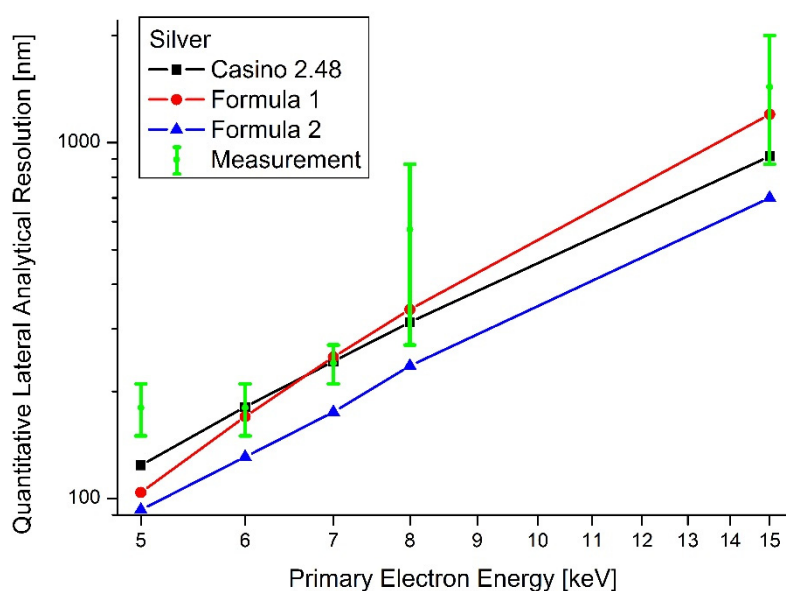
The graph elucidates the improvement of the resolution with decreasing excitation energy due to the decreasing source volume of emitted X-rays. Another remarkable result is the good correlation between measurement and Monte Carlo simulation, except at the primary electron energy of 3 keV for which the overvoltage is below 2. The reasons for this discrepancy are not clear.

The calculated values deviated from the measurements in the same manner at 3 keV. For higher electron energies there is the tendency that eq. (1) predicts a little bit too large values and eq. (2) a little bit too low values.

In the case of silver (table 4 and figure 9) the results from measurement and Monte Carlo simulation coincide as well as for aluminium. In addition, the calculated value from eq. (1) are in good agreement with both whereas eq. (2) predicts rather to small values again.

**Table 4.** Comparison of simulated, calculated and measured quantitative lateral resolutions for Ag and different primary electron energies.

Electron energy	Lateral resolution from MC simulation [nm]	$R_x$ [nm]	$Z_m$ [nm]	Calculated lateral resolution $R_s$ with formula (1) [nm]	Calculated lateral resolution $R_s$ with formula (2) [nm]	Measured lateral resolution [nm]
15 keV	916	670	70	1201	700	870-2000
8 keV	313	193	24	340	236	270-870
7 keV	243	142	18	250	175	210-270
5 keV	181	96	13	170	131	150-210
3 keV	124	55	7	104	93	150-210

**Figure 9.** Comparison of the simulated, calculated and measured quantitative lateral resolutions for Ag and different primary electron energies.

Nevertheless, the discrepancy between simulation and calculation to measurement are once more obvious for the lowest primary electron energy. Since the electron optical properties and the stability of the used microprobe are perfect for the electron energy of 5 keV, as can be seen from the consistent experimental data for 5 keV in the aluminium measurements, there is no reason to doubt the accurateness of the measurements. Therefore, the most probable reason for the discrepancy is the wrong estimation of the scattering volume due to inaccurate values of  $R_x$  and  $Z_m$  in the calculation and the scattering cross-sections in the Monte Carlo simulations which show up more clear if the primary electron energy is close to the ionisation energy with an overvoltage well below or close to 2.

### 2.5. $Z$ -dependence of the quantitative lateral resolution

From the results of this and the previous paper [8] the atomic number ( $Z$ )-dependence of the quantitative lateral resolution can be derived for the first time. Figure 10 shows this  $Z$ -dependence for different primary electron energies.

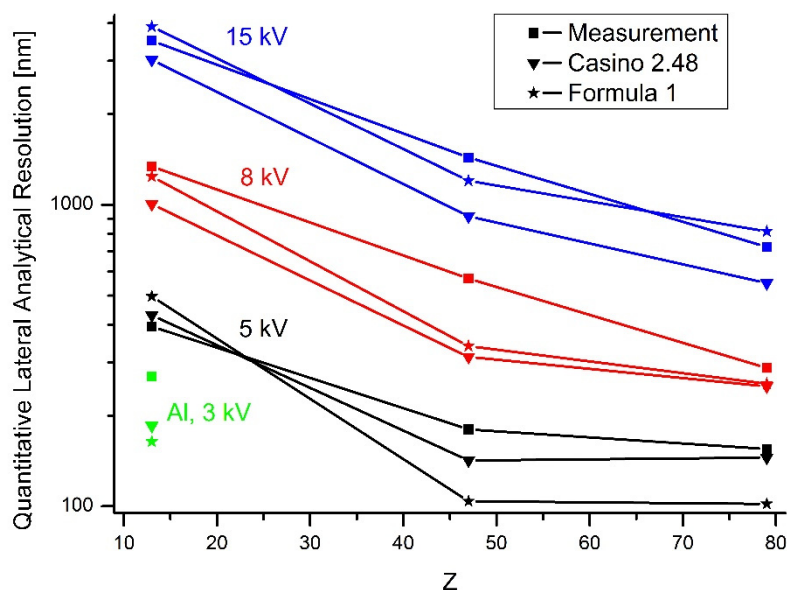


**Figure 10.** Quantitative lateral analytical resolution as a function of atomic number at 15, 8 and 5 keV primary electron energy at suitable measurement conditions.

On one hand the resolution improves with decreasing energy, due to the reduction of the electron interaction volume inside the material. Obviously, the reduction of the interaction volume is not compensated completely by the increase of the beam diameter at low primary electron energies. On the other hand, the resolution becomes worse with lower atomic number owing to the lower density of the material and hence the increasing spread of electrons. However, at 5 keV there is no significant difference between Au (79) and Ag (47). For the Ag measurement, the overvoltage is low in relation to the critical ionisation energy of the Ag-L $\alpha$  X-ray line at 3.352 keV. Hence, the range of excited Ag-L $\alpha$  X-rays is small. For the Au measurement, the Au-M $\alpha$  X-ray line was used (ionisation energy of 2.31 keV) for which the overvoltage is larger. Therefore, the decrease of the X-ray emitting volume due to higher Z is compensated by its increase due to the higher overvoltage. It should be noted again that the further decrease of the primary electron energy would on one hand increase the resolution but on the other hand worsens the counting statistics to unusable values. In addition, it should be kept in mind that the shown Z-dependence relies on different X-ray lines with different absorption properties. The aim of this investigation is rather to determine the thickness of layers for which an accurate element quantification is possible than to compare the lateral resolution for different X-ray lines.

### 3. Conclusion

In this paper measurements of the quantitative lateral analytical resolutions at thin test specimens with usable beam currents and acquisition times are presented. The experiments are accomplished at metallic layers with different thicknesses and different atomic numbers. For silver the lowest quantitative lateral resolution in the range of 150 to 210 nm is obtained for 5 keV and for aluminium 260 to 280 nm for 3 keV. These results are in good agreement with those previously obtained at gold (140 to 170 nm at 5 keV).

The experimental results are in accordance with Monte Carlo simulations and analytical calculations for most primary electron energies, but differ significantly for low energies for which the overvoltage is below or close to two. The cause for this discrepancy is not clear yet and has to be clarified by further investigations, in particular because the best quantitative analytical resolution is obtained at low energies for which the discrepancy is the largest.

### Acknowledgements

The financial support by the Europäische Fonds für Regionale Entwicklung (EFRE) within the projects "Nano-Analytiklabor" and "Nano-Werkbank" is gratefully acknowledged. We thank Xavier Llovet for fruitful discussion and the support in applying eq. (1).

### References

- [ 1 ] Berger D and Nissen J 2014 *IOP Conf. Ser.: Mater. Sci. Engng.* **55** 012002
- [ 2 ] Berger D and Galbert F 2011 *MC2011 Conf. Proc.* (Kiel, Germany) ISBN 978-3-00-033910-3 IM7.P208
- [ 3 ] Carpenter P K and Jolliff B L 2015 *Microsc. Microanal.* **21** (Suppl. 3) 1443-1444
- [ 4 ] Drouin D, et al. 2007 *Scanning* **29** 92-101
- [ 5 ] Merlet C and Llovet X 2012 *IOP Conf. Ser.: Mater. Sci. Engng.* **32** 012016
- [ 6 ] Willich P and Bethke R 1996 *Mikrochim Acta Suppl.* **13** 631
- [ 7 ] Merlet C 1994 *Mikrochim. Acta* **114/115** 363-376
- [ 8 ] Berger D and Nissen J 2016 *IOP Conf. Ser.: Mater. Sci. Engng.* **109** 012001